Contents lists available at ScienceDirect

Arabian Journal of Chemistry

journal homepage: www.ksu.edu.sa

Improving flowability of the propellant prepared by solventless extrusion process by integration dendrimer and investigation on its thermal, sensitivity, and combustion features

Qian Chen, Zhitao Liu *, Yao Zhu, Jianwei Zhang, Ling Chen, Bin Xu, Jing Yang, You Fu, Xijin Wang, Feiyun Chen, Xin Liao *

School of Chemistry and Chemical Engineering, Nanjing University of Science and Technology, Nanjing, Jiangsu 210094, China
Key Laboratory of Special Energy Materials, Ministry of Education, Nanjing, Jiangsu 210094, China

ARTICLE INFO

Keywords:
Propellant
Dendrimer
Solventless extrusion
Rheological properties
Sensitivity
Combustion

ABSTRACT

A mixed nitrate ester propellant composed of nitrocellulose, nitroglycerin, triethylene glycol dinitrate, and dendrimer DP-2 was studied to explore the effects of DP-2 on the rheological properties of the propellant during the solventless extrusion process. The results showed that the apparent shear viscosity of the propellant decreased gradually with the increased mass fraction of the DP-2 from 0 wt% to 2 wt%. Additionally, it was evident that the inclusion of 0.5 wt% DP-2 leads to a notable decrease in both the apparent shear viscosity of the propellant and the torque of screw by over 50%. However, in contrast to the change in fluidity observed from 0 wt% to 0.5 wt%, the enhancement trend of propellant fluidity becomes less significant as the DP-2 content continues to increase. The effects of DP-2 on thermal properties, chemical stability, mechanical sensitivity, mechanical property, and combustion behavior of the propellant were comprehensively assessed. The results demonstrated that DP-2 exhibited promising potential as a flow modification additive for the manufacture of the propellant by solventless extrusion process.

1. Introduction

In the domain of energetic materials, propellant, as the main source of power for conventional weapons, has a huge demand in warfare. As science and technology continue to advance, modern warfare requires artillery weapons with greater range and caliber. Consequently, research on large thick propellants has become a prominent development trend to meet the demands of larger caliber weapon charges. Currently, the traditional manufacturing process of double-base propellant is mainly divided into solvent extrusion and solventless extrusion processes. For the solvent extrusion process, the shape of the propellant grains obtained by extrusion molding will shrink due to the volatilization of residual ethanol and acetone. In addition, ethanol and acetone are difficult to drive away cleanly, especially for large thick propellant. As a result, the consistency of the propellant quality is dissatisfied. On the contrary, the solventless extrusion process with the help of high-temperature plasticization, the shape and size of the propellant obtained by extrusion molding are consistent, and the quality consistency is high, which has certain advantages compared with the solvent extrusion process. However, there is still a high safety risk in the preparation of the propellant by solventless extrusion process at present, which mainly comes from two aspects. One is the thermal stimulation, which arises not only from the high-temperature environment required for propellant solvent-free extrusion preparation but also from the significant heat generated during fluid shear flow. The other is the mechanical stimulation caused by the friction between the propellant paste and the metal wall surface during the extrusion process due to the high pressure caused by the high viscosity of the propellant (Zhang, 1997). Therefore, enhancing the production safety of solventless extrusion process for the propellant is a problem that needs to be solved urgently at this stage. Due to the poor fluidity of the propellant, improving its processing fluidity and thus reducing the high temperature and high-pressure environment required for the preparation of the propellant by solventless extrusion process is the main means to enhance the production safety. Hence, the search for efficient flow modification additives has become the key to addressing the issue.

Peer review under responsibility of King Saud University.
* Corresponding authors at: School of Chemistry and Chemical Engineering, Nan-jing University of Science and Technology, Nanjing, Jiangsu 210094, China.
E-mail addresses: liuzhitao331@163.com (Z. Liu), liaoxin331@163.com (X. Liao).

https://doi.org/10.1016/j.arabjc.2023.105574
Received 13 June 2023; Accepted 16 December 2023
Available online 21 December 2023

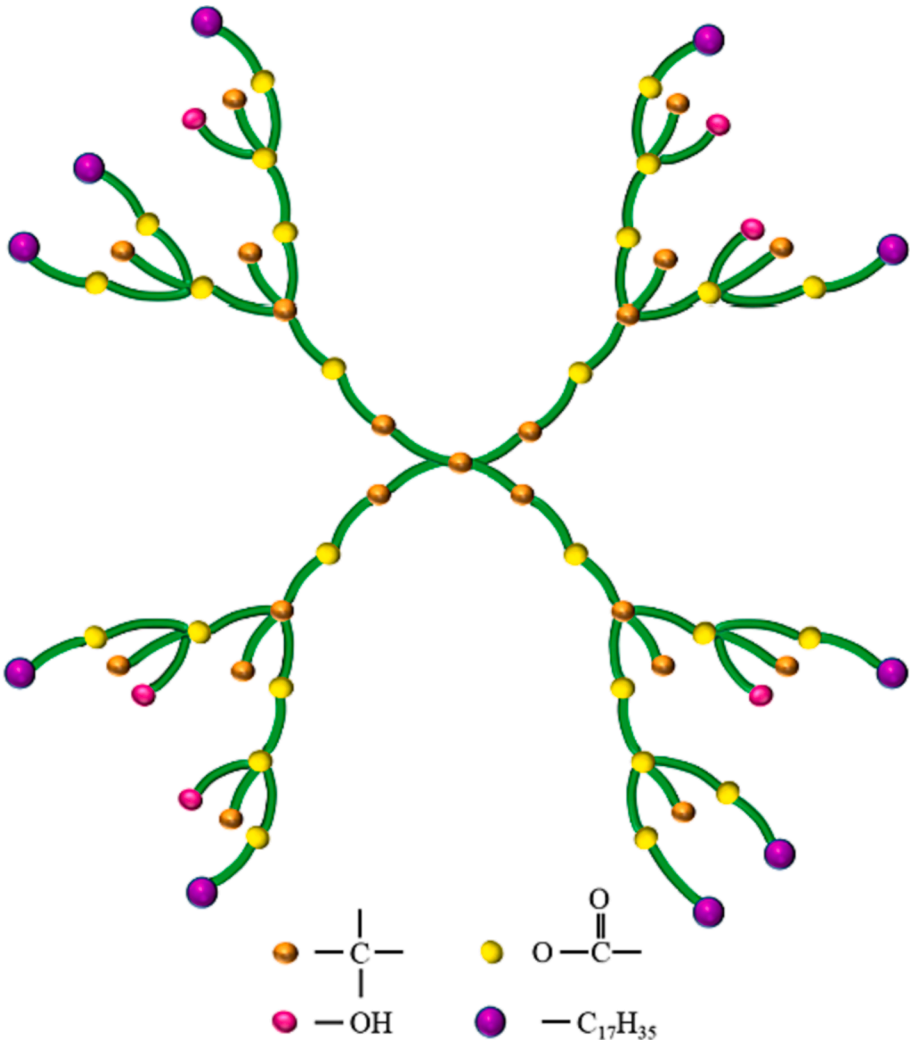

Fig. 1. Structure schematic diagram of DP-2.

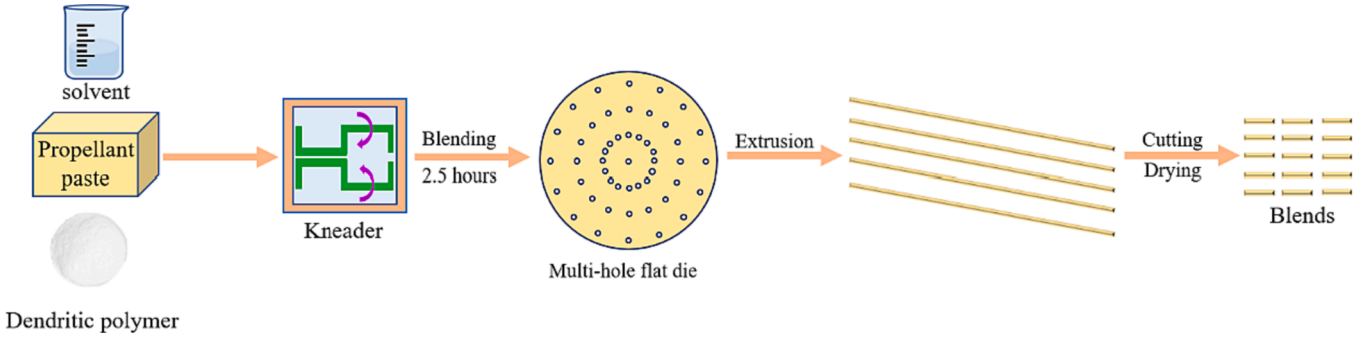

Fig. 2. Blends preparation.

Compounds with highly branched structures, like dendrimers, are considered as flow processing aids due to their non-entanglement between molecules (Merino et al., 2001), low viscosity, and good compatibility, which have attracted widespread attention in recent decades. In theoretical calculations, Hajizadeh et al. used non-equilibrium molecular dynamics (NEMD) methods to simulate the structure and rheological properties of linear polymer chains and dendritic polymer blends, and the results showed that dendritic macromolecules can increase the free volume of the blends and thus reduce the shear viscosity and first tensile viscosity of the blends (Hajizadeh et al., 2014; Hajizadeh et al., 2015). There are also many practical applications in various polymer processing, for instance, Kang et al. blended a small amount of dendrimer with high-viscosity polyamide 6 to improve the flowability of the polymer by reducing the viscosity, and the results showed that the flowability of the blended system of polyamide 6 and dendrimer increased significantly with the increase of the dendrimer content (Kang and Kim, 2021). Besides, Zhang et al. added self-prepared azide hyperbranched copolymers to GAP-ETPE propellant system to improve the process performance, and the results showed that the azide hyperbranched polymers could effectively reduce the consistency coefficient

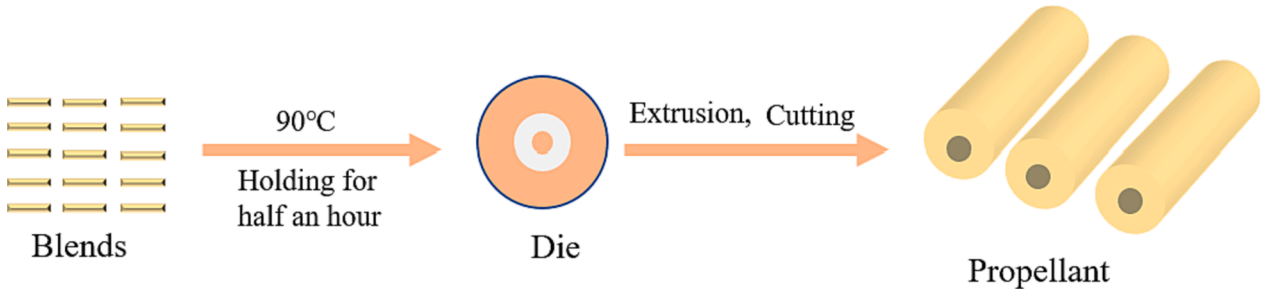

Fig. 3. Propellant preparation by solventless extrusion.

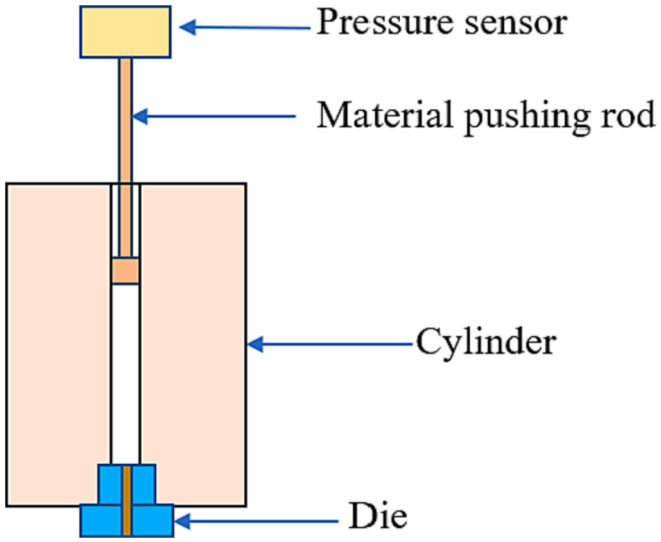

Fig. 4. Explosion-proof capillary rheometer.

and viscous flow activation energy of GAP-ETPE system (Zhang and Luo, 2021). Hong et al. investigated the use of hyperbranched polymers as processing aids for linear low-density polyethylene (LLDPE), and the results showed that the addition of hyperbranched polymers significantly reduced the power requirement of the extruder, and the flow rate of the blends was higher than that of pure LLDPE and LLDPE-paraffin blends at the same extrusion speed. And the melt fracture and shark-skin problems due to excessive LLDPE viscosity were solved (Hong et al., 1999). Moreover, HAN et al. studied the melt flow behavior of blended systems of polyamide 6 and hyperbranched polymers, and the results showed that the addition of a small amount of HBP could significantly improve the flow index of the blended system (Han et al., 2010). In solution systems, Nuenz et al. studied the rheological properties of different generations of hyperbranched polyesters in 1-methyl-2-pyrrolidone solvent and their blends with poly (2-hydroxyethyl methacrylate), and the results showed that the introduction of hyperbranched polymers led to a significant reduction in the viscosity of the blends (Nunez et al., 2000).

The aim of this study was to enhance the fluidity and safety in propellant preparation by solventless extrusion process. To accomplish this, a small quantity of dendrimer was incorporated into the mixed nitrate propellant formulation, resulting in the development of propellant with exceptional fluidity. The effects of the addition of dendrimer on the thermal properties, chemical stability, rheological properties, mechanical property, mechanical sensitivities, and combustion behavior of the propellant were investigated.

2. Experiment

2.1. Materials

The dendrimer DP-2 was purchased from Weihai CY Dendrimer Technology, China. It is a dendritic polyester polyol structure, and the chemical formula is $C_{245}H_{448}O_{50}$ with a molecular weight of 4194.23 and a melting point of 39 °C. The structure schematic diagram of DP-2 was shown in Fig. 1. The propellant paste was obtained from Sichuan Nitrocellulose Co. Ltd. Which is composed of 60 wt% nitrocellulose (NC), 15.5 wt% nitroglycerine (NG), 21.5 wt% triethylene glycol dinitrate (TEGDN), 2.0 wt% Dimethyl phenyl Urea (C_2) and 1.0 wt% TiO_2. Analytical reagent grade ethanol and acetone were purchased from Sinopharm Chemical Reagent Co., Ltd. All chemicals were used as obtained without any further purification or modification.

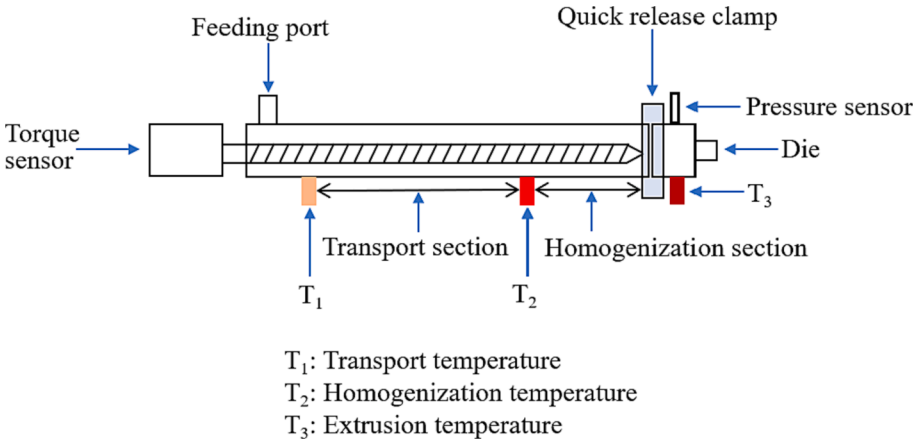

Fig. 5. Explosion-proof torque rheometer.

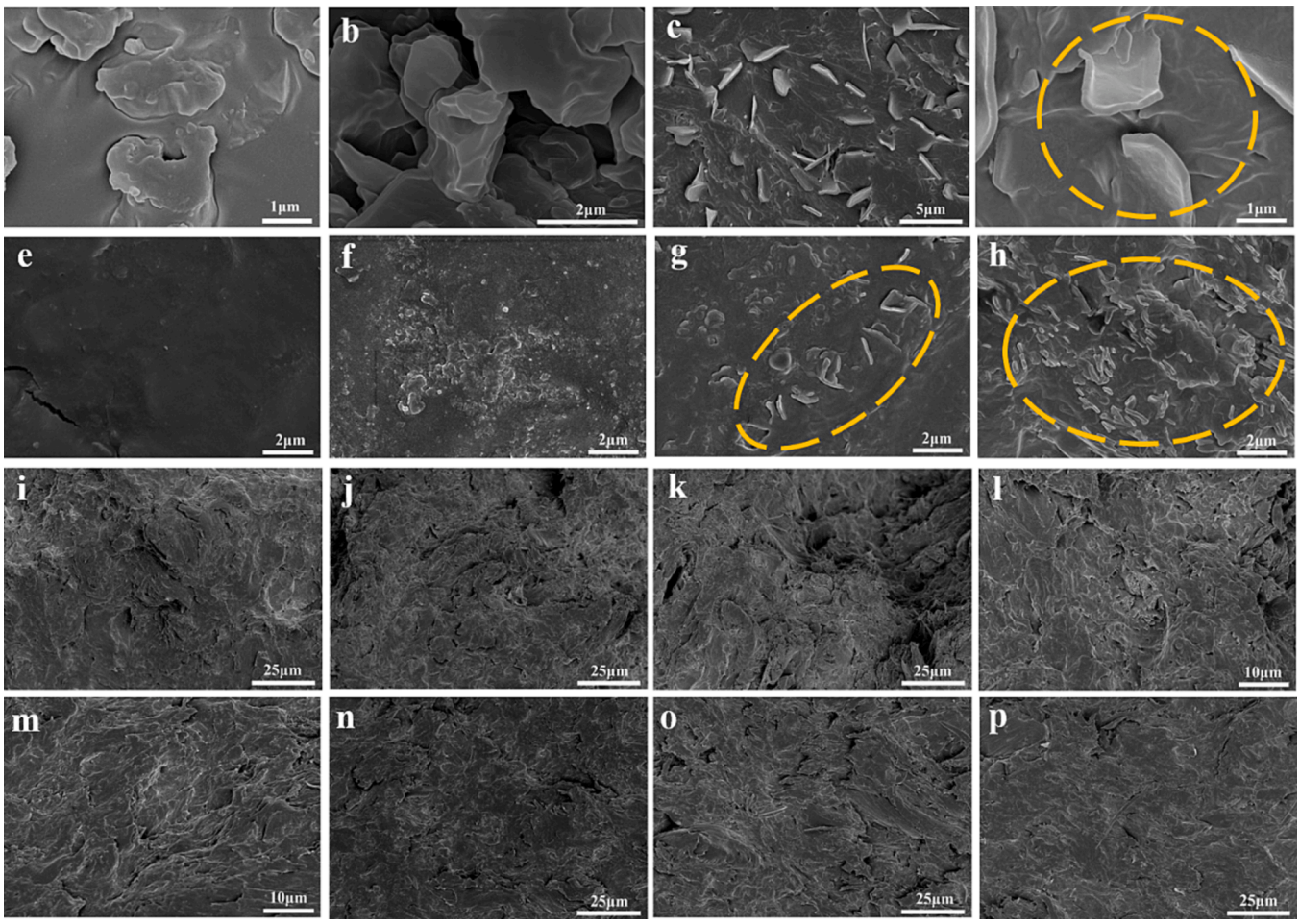

Fig. 6. SEM images of DP-2 and the propellant containing DP-2 (a-d: DP-2, e-h: surface of the propellant, and i-p: internal of the propellant).

2.2. Samples preparation

2.2.1. Blends preparation

The preparation process of the propellant blends containing DP-2 was displayed in Fig. 2. First, the dried propellant paste and a certain amount of DP-2 were added in a kneader. Meanwhile, a mixed solvent of acetone and ethanol with a volume ratio of 2:3 was poured into the kneader. Then the uniform distribution dough was obtained after stirring for about 2.5 h. Subsequently, the dough was added into a barrel with a multi-hole flat die. Many blend strands with a 1.5 mm diameter were extruded from the mold by a plunger type hydraulic press. These strands were cut into 10–15 mm lengths and placed for 2 days. Finally, these blends were dried at 45 °C for 6 days. Four kinds of blends were prepared by changing the adding content of DP-2 and the adding content of DP-2 was 0 wt%, 0.5 wt%, 1 wt%, and 2 wt%, respectively.

2.2.2. Propellant preparation by solventless extrusion

The blends were held at 90 °C for half an hour and then the single-hole propellant was extruded through a hydraulic press for testing. The diagram illustration of the preparation process was displayed in Fig. 3.

2.3. Characterization

2.3.1. Morphology characterization

The effect of dendrimer filler on the morphology of the propellant matrix was investigated by scanning electron microscopy (HITACHI UHR FE-SEM SU8200). To ensure conductivity under the electron beam, the glass slides containing samples were coated with a layer of gold. The test was conducted at 5KV.

2.3.2. Thermal properties

The thermal performance of the propellant matrix containing DP-2 was studied via a differential scanning calorimeter (DSC, NETZSCH 204F 1 instruments, Germany). The DSC instrument was calibrated with In, Sn, Zn and CsCl standards. The sample, weighing approximately 1.0 mg, was placed inside an aluminum crucible. The heating rate was (5, 10, 15, 20) °C min^{-1}, the temperature range was from 25 °C to 300 °C, and the scavenging gas and the protective gas were nitrogen at a flow rate of 40 mL min^{-1} and 60 mL min^{-1}, respectively.

TG-DSC-FTIR analysis was used to study the thermal decomposition weight loss behavior of the samples as well as the gaseous products during the thermal decomposition of the samples by Mettle-Toledo TGA/DSC 3 and Nicolet Is50 (Fu et al., 2022). Approximately 1.0 mg of sample was put in a ceramic crucible and then heated from 50 °C to 400 °C at a heating rate of 10 °C min^{-1}. High-purity argon was used as the purge gas with a gas flow rate of 20 mL min^{-1}. IR spectra in the range 4000–525 cm^{-1} were captured by a specific detector with a resolution of 4 cm^{-1}.

2.3.3. Chemical stability

Chemical stability is a crucial factor in evaluating the storage life-span of munitions, as thermal decomposition of artillery propellant in high temperature environments can potentially lead to accidents. Therefore, it is imperative to conduct thorough chemical stability assessments, especially when preparing the propellant through solventless

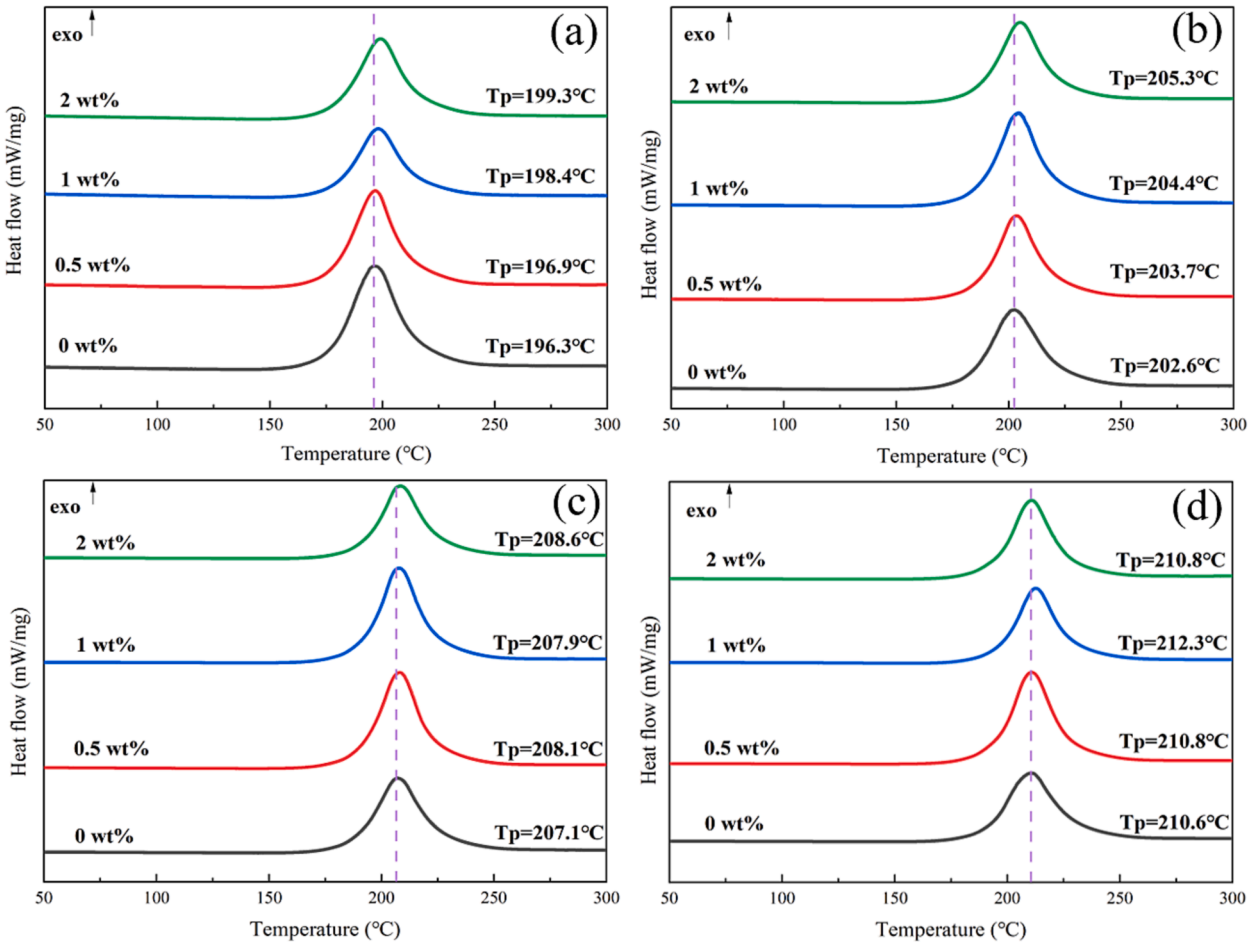

Fig. 7. DSC curves of the propellant at different heating rates(a:5 k·min^{-1}, b:10 k·min^{-1}, c:15 k·min^{-1}, d:20 k·min^{-1}).

extrusion process that require high-temperature conditions (de Klerk, 2015).

The chemical stability of samples was tested by OZM RESEARCH MVT 01, Czech. Referring to the GJB 770B-2005 method 503.3 (Li et al., 2023). The time for the methyl violet test paper turned from purple to orange by the gas released by the thermal decomposition of the 2.5 g sample in the test tube at 120 °C was evaluated.

2.3.4. Mechanical sensitivity

The propellant can ignite and explode under mechanical stimulation, such as impact, friction, and electrostatic discharge (Wang et al., 2021). Especially during the extrusion of the propellant, friction between the propellant paste and the metal wall surface will inevitably occur (Carter, 1988; Dombe et al., 2015; Kowalczyk et al., 2007). The mechanical sensitivity test is a widely used approach for assessing the safety of samples.

The impact, friction, and electrostatic discharge sensitivity were separately tested by OZM RESEARCH BFH12, OZM RESEARCH FSKM10, and OZM RESEARCH Xspark10. In at least six tests, the minimum stimulus energy or load for at least one test to explode was recorded as the ultimate impact energy, the ultimate electrostatic ignition energy, and the ultimate friction load, respectively.

2.3.5. Rheological properties

So far, the main production methods of the propellant by solventless extrusion process are plunger extrusion and screw extrusion. The capillary rheometer and torque rheometer were employed to assess the enhancement of sample fluidity, aiming to demonstrate the processability of these two processes (Fleming et al., 2022).

The apparent viscosity (η) of blends at different temperatures and shear rates (γ) was measured by an explosion-proof capillary rheometer (MLW-90B, Changchun Intelligent Instrument Equipment CO., Ltd, Fig. 4). The torque of the screw during extrusion of a single-screw extruder at different temperatures was observed by an explosion-proof torque rheometer (ZJL-FB-200, Changchun Intelligent Instrument Equipment CO., Ltd, Fig. 5).

2.3.6. Mechanical properties

Due to the complex kinetic environment in which the propellant is located in the gun chambers, the mechanical properties of the propellant will directly affect its combustion stability. Therefore, the study of the mechanical properties of the propellant is essential to evaluate its quality system (Chen et al., 2022; Shen et al., 2019). The anti-impact strengthen of the propellant was performed with a simple beam impact tester at −40 °C. (GDW-100, Changchun Intelligent Instrument Equipment CO., Ltd.).

2.3.7. Combustion characteristics

As the power source of artillery, the burning properties of the propellant are important research object. As an inert additive material, DP-2 is added to the propellant, which will inevitably have a certain impact on the combustion features of the propellant.

The high-pressure burning of the propellant was analyzed by a closed bomb with a volume of 100 cm^3. Besides, since the initial temperature of the propellant has a direct influence on its combustion features, the combustion features of the propellant under different initial temperature conditions (-40 °C, 20 °C, 50 °C) were researched.

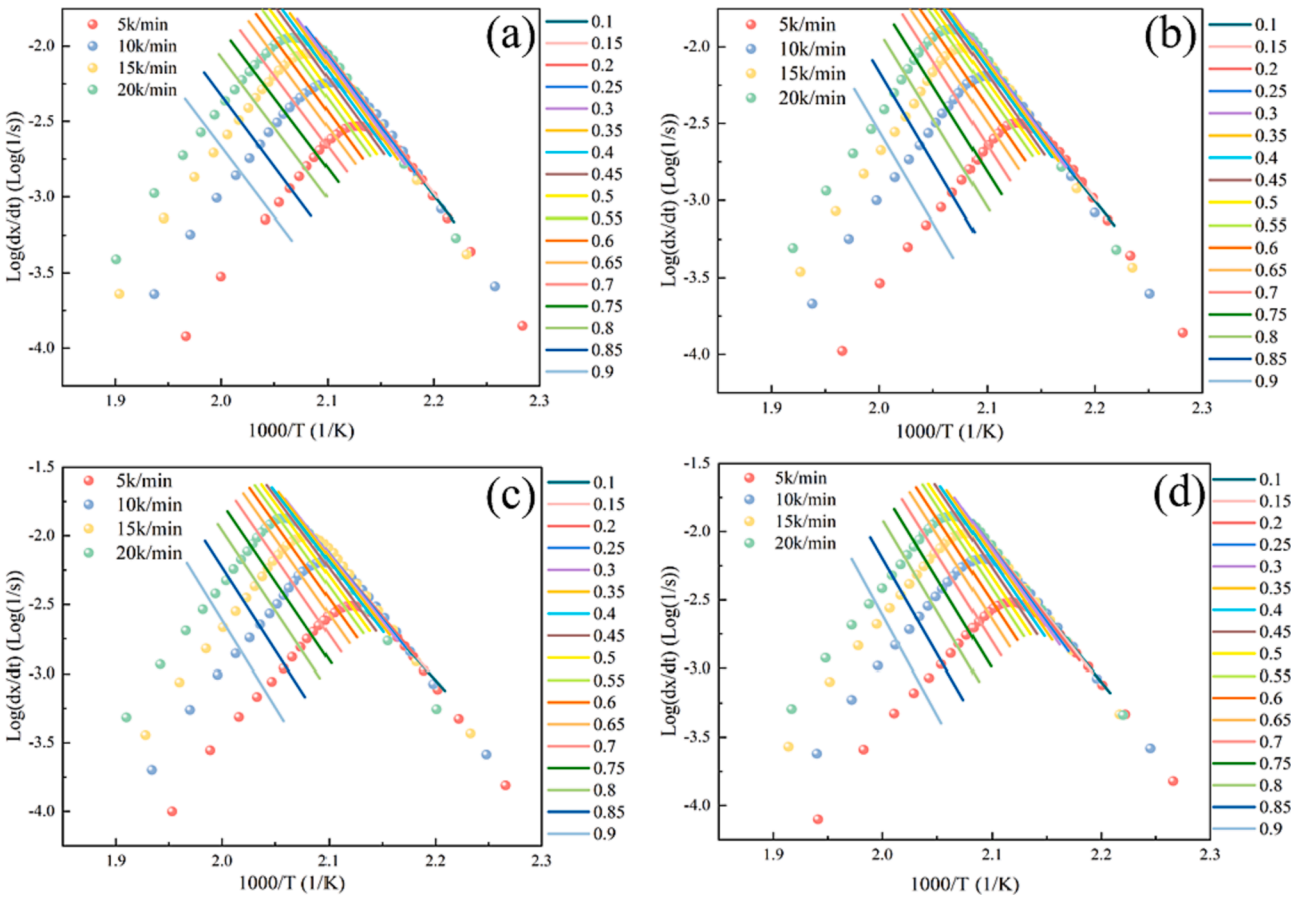

Fig. 8. Friedman plots of the propellant with different mass fraction of DP-2 (a:0 wt%, b:0.5 wt%, c:1 wt%, d:2 wt%).

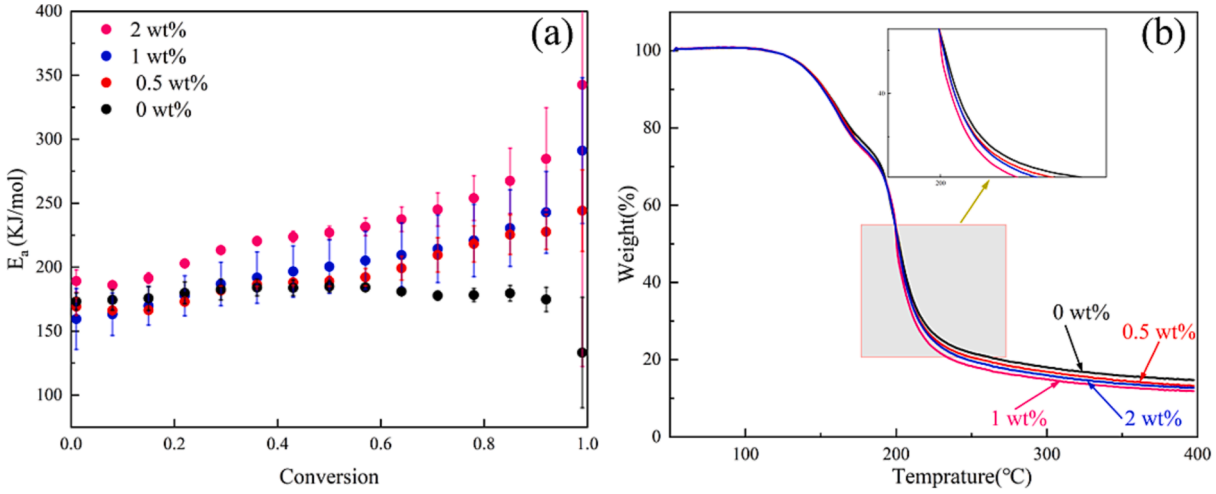

Fig. 9. (a) E_a at different conversion (α) and (b) TG curves of the propellant with different mass fraction of DP-2 at the heating rate of 10 K min^{-1}.

3. Results and discussion

3.1. Morphology and microstructure analysis

In Fig. 6, Fig. 6**a-b** presents the initial morphology of DP-2 samples, while Fig. 6**c-d** illustrated the flake-like shape observed after melting and cooling DP-2 to room temperature. Fig. 6**c-h** exhibited the surfaces of propellant samples with varying mass fractions of DP-2. Notably, in Fig. 6**g and 6 h** (with DP-2 content at 1 wt% and 2 wt%, respectively), clear evidence of DP-2 presence on the propellant surface was observed. Cross-sections of propellant samples containing different mass fractions of DP-2 were shown in Fig. 6**i-l**, while longitudinal sections were displayed in Fig. 6**m-p**. The uniformity of the internal structure indicated excellent compatibility as DP-2 was uniformly dispersed within the propellant matrix without significant phase separation.

3.2. Thermal behavior analysis

Thermal property is a vatial parameter to the comprehensive performance of the propellant. In Fig. 7, the DSC curves of samples are

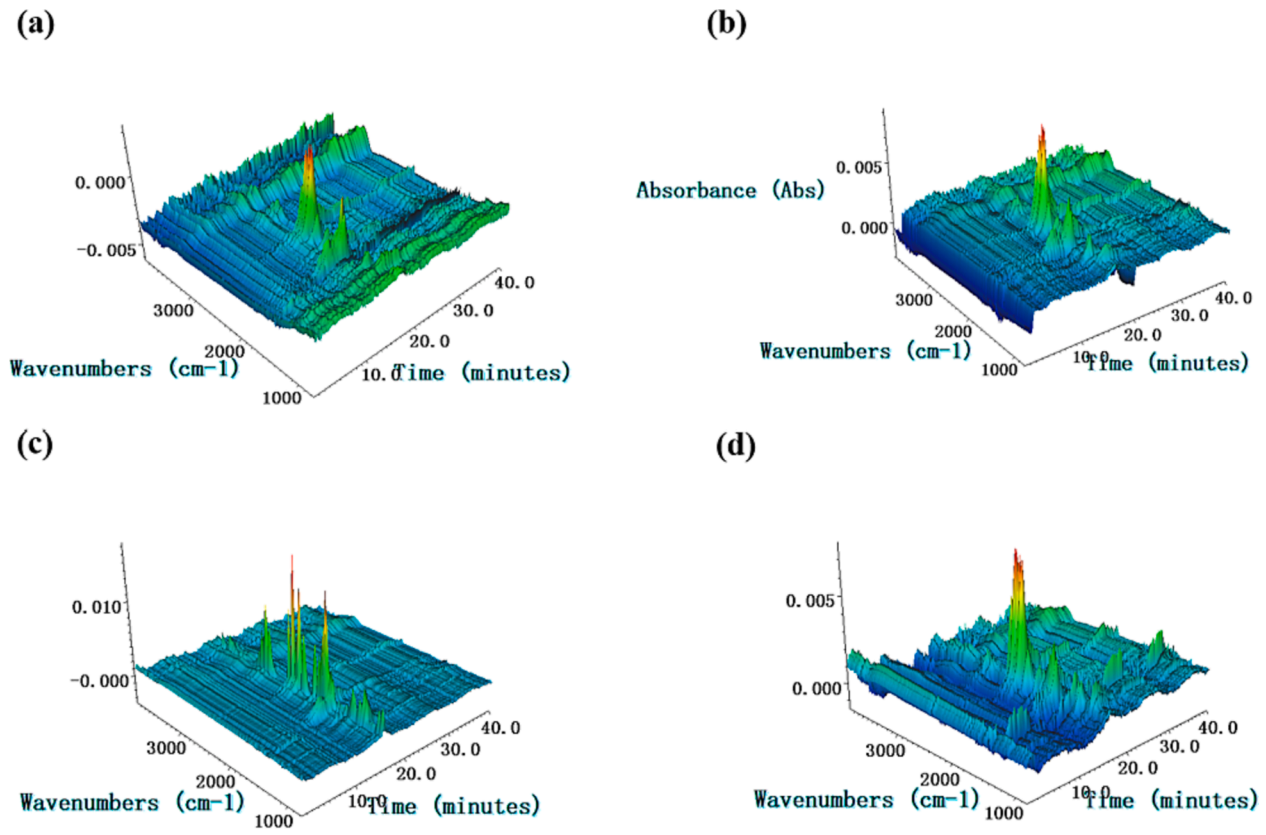

Fig. 10. The 3D images of FTIR spectra of pyrolysis gases in the thermal decomposition process of the propellant with different mass fraction of DP-2 (a:0 wt%, b:0.5 wt%, c:1 wt%, d:2 wt%).

carried ot under different heating rates conditions. According to the results of temperature peak, it can be obtained that the addition of DP-2 could delay the thermal decomposition process of the propellant. As shown in Fig. 7**a**, at the heating rate of 5 K min^{-1}, the decomposition peak temperature of the propellant increased from 196.3 °C to 199.3 °C with the increase of DP-2 content. At the same time, with the increase of the heating rate, the delay effect decreased gradually.

Further, the thermal decomposition dynamic was investigated to study the effect of DP-2 on the propellant. The activation energy (E_a) during the thermal decomposition of each sample was calculated by the Friedman method. The Friedman method is one of the "Model-free" methods that can determine the activation energy without a precise knowledge of reaction mechanism (Zhang et al., 2023). Friedman's equation is as **Equation (1)**.

$$\ln\left(\frac{d\alpha}{dt}\right)_{\alpha,i} = \ln[f(\alpha)A_\alpha] - \frac{E_a}{RT_{\alpha,i}} \quad (1)$$

Where, the subscripts i and α denote the different heating rates and the conversion. The plot of *Log (dα/dt)* versus *1000/T* at constant α values gives a family of straight lines with slope $-E_a/R$ by the kinetic software.

The Friedman plots were shown in Fig. 8. The correlation coefficients of the Friedman method were all greater than 0.99, indicating that the Friedman method had good accuracy. Fig. 9**a** showed the E_a at different conversion rates (α). Theoretically, during the sophisticated reaction process, the E_a varies with α. This relationship between them is related to the overlap of many solid-phase reactions occurring during the decomposition process. For complicated non-homogeneous reactions, the actual measured E_a is determined by the relationship of each reaction step and its relative contribution to the overall reaction. In this study, it could be seen that the addition of DP-2 caused a significant change in the trend of E_a in the interval of 0.40–1.0 for the α. In this interval, E_a of blank sample showed an overall decreasing trend, while the other samples showed gradually increased trend. The results demonstrated that DP-2 participated in the thermal decomposition reaction of the propellant.

The TG-DSC-FTIR test was used to further investigate the involvement of DP-2 in the thermal decomposition process of the propellant. The TG curves of the samples at the heating rate of 10 K·min^{-1} were shown in Fig. 9**b**. Two stages could be seen from the TG curves. In the first stage (126.2 °C-185.5 °C), the volatilization and thermal decomposition of NG and TEGDN were occurred, In the second stage (185.5 °C-400 °C), the thermal decomposition of NC was occurred. The trend of change in TG curves and residual amount of different samples during the thermal decomposition process indicated that DP-2 has little impact on the volatilization and thermal decomposition of NG and TEGDN. However, it appeared that DP-2 may enhance the thermal decomposition process of NC's skeleton in the second stage, particularly when its content was 1 %.

Based on the analysis results of DSC curves, the variation trend of *Ea* and TG curves of samples, we found that DP-2 had no effect on the plasticizer (NG and TEGDN) in the sample, but promoted the decomposition of the binder (NC). For this reason, the decomposition gaseous products were collected and detected by IR and its 3D images as well as the corresponding absorption peaks was obtained, as shown in Fig. 10 and Fig. 11.

As displayed, the infrared absorption peaks of NO_2 (1636 cm^{-1}, 1593 cm^{-1}) can be observed at 159.0 °C, which indicated that -O-NO_2 bond of NG and TEGDN was broken firstly, forming –HC = O group and NO_2. Subsequently, the infrared absorption peaks of CO_2 (2383 cm^{-1}, 2309 cm^{-1}), N_2O (2241 cm^{-1}, 2190 cm^{-1}), CO (2105 cm^{-1}) and NO (1912 cm^{-1}, 1845 cm^{-1}) can be observed at 159.0 °C-199.5 °C. The thermal decomposition paths of samples with different contents of DP-2 were found to be essentially identical in this stage, thereby reaffirming

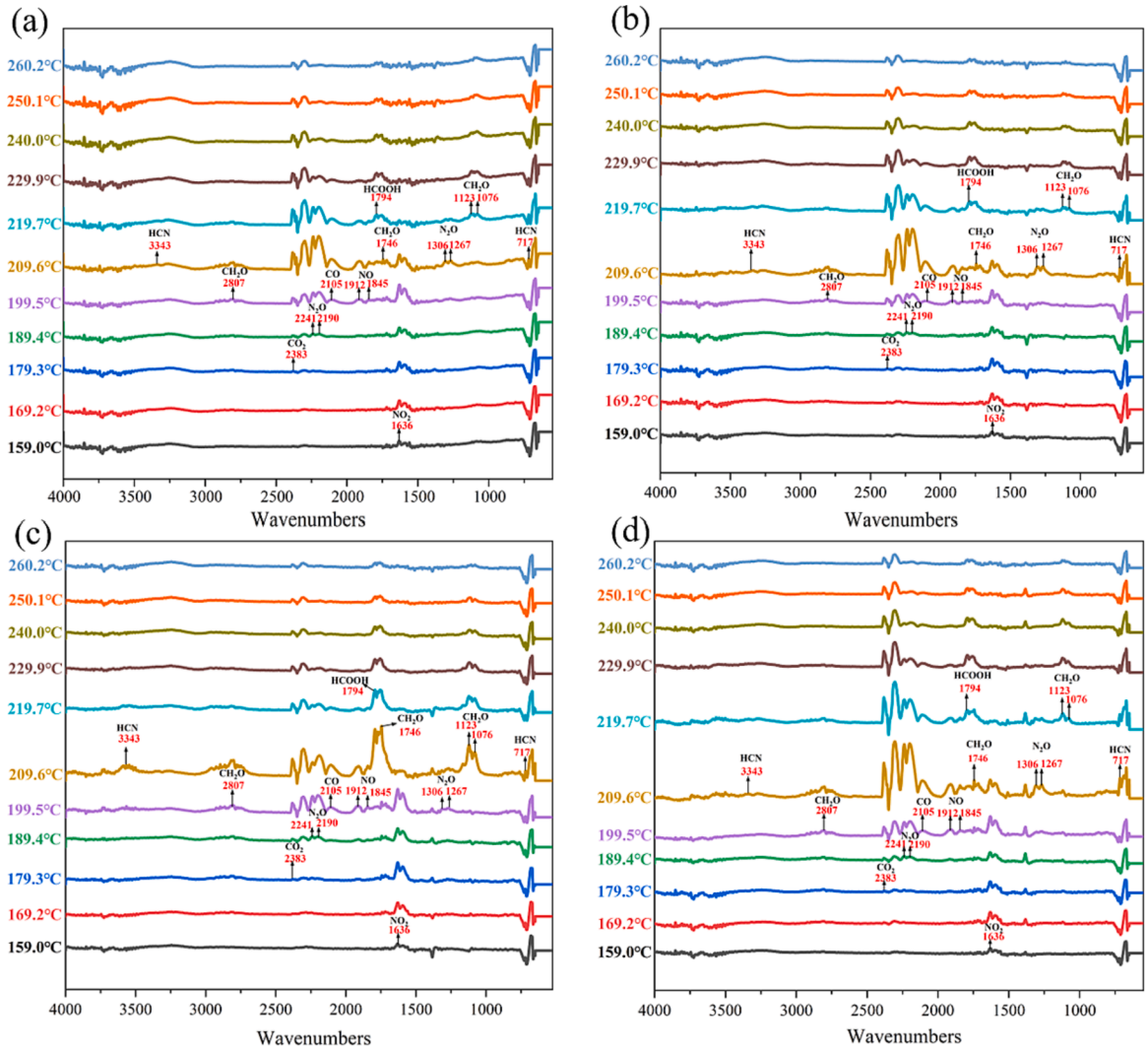

Fig. 11. The FTIR spectra of pyrolysis gases in the thermal decomposition process of the propellant with different mass fraction of DP-2 (a:0 wt%, b:0.5 wt%, c:1 wt %, d:2 wt%).

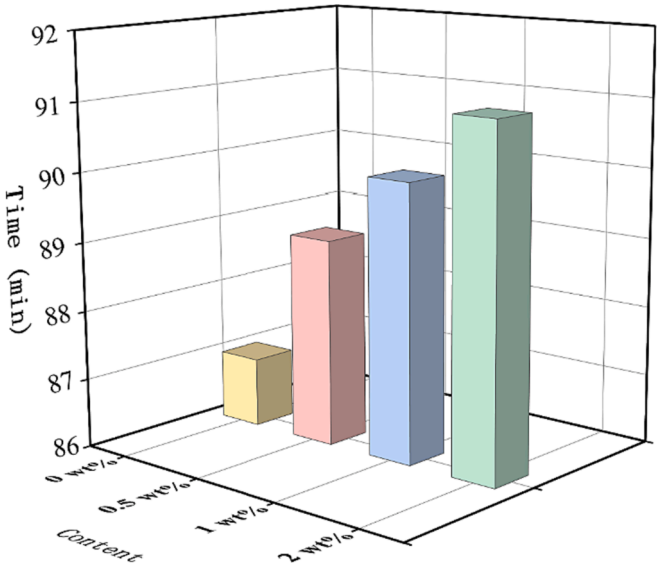

Fig. 12. Time for the test paper to turn completely orange for the propellant with different mass fraction of DP-2.

Table 1
The results of mechanical sensitivity tests.

DP-2 content (wt%)	Ultimate impact energy (J)	Ultimate electrostatic ignition energy (J)	Ultimate friction load (N)
0	4	26.95	216
0.5	4	35.20	216
1	4	55.00	240
2	3	55.00	252

the negligible impact of DP-2 on the thermal decomposition of NG and TEGDN. Meanwhile, this also ensured the safety of the processing process after the addition of DP-2. After then, the products of CH_2O (2807 cm^{-1}, 1746 cm^{-1}, 1123 cm^{-1}, 1073 cm^{-1}), HCOOH (1794 cm^{-1}) and HCN (715 cm^{-1}, 3343 cm^{-1}) were released further. However, with the increase of DP-2 content in the samples, the characteristic signals of CH_2O and HCOOH were enhanced, which further proved that DP-2 accelerated the decomposition of NC skeleton.

3.3. Chemical stability analysis

The increase in DP-2 content, as depicted in Fig. 12 under the specified test conditions, resulted in a gradual prolongation of the time

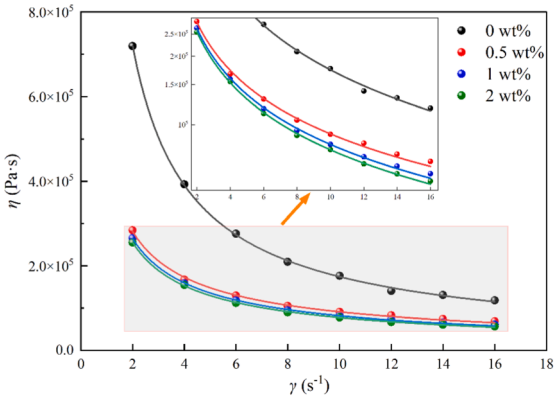

Fig. 13. The apparent shear viscosity of the propellant blends at 70 °C at different shear rates.

taken for methyl violet test paper to transition from purple to completely orange, ranging from 87 min to 91 min. Furthermore, no instances of explosion or combustion were observed in the propellant samples following exposure to a temperature of 120 °C for a duration of 5 h. It indicated that DP-2 can effectively enhance the chemical stability of the propellant. This was consistent with the DSC test results.

3.4. Mechanical sensitivity analysis

The results of mechanical sensitivity tests were shown in Table 1. The impact sensitivity of the propellant was not significantly affected by DP-2 content ranging from 0 wt% to 1 wt%, but exhibited an increase when the addition content of DP-2 reached 2.0 wt%. From the perspective of electrostatic sensitivity, there was an obvious decreasing tendency in the wake of the increased content of DP-2 from 0 wt% to 1 wt%. When the content of DP-2 reached 2 wt%, there was no change in electrostatic sensitivity. The DP-2 content of 0.5 wt% has no effect on the friction sensitivity of the propellant. When the content of DP-2 continued to increase from 0.5 wt% to 2 wt%, a significant decrease in the friction sensitivity could be clearly found. As a well-known fact that the addition of inert functional additives would inevitably reduce the energy performance of energetic materials from a certain degree to desensitization. In addition, DP-2 may effectively conduct heat and electrostatic forces in the propellant matrix, preventing the accumulation of heat and electrostatic on the inner of the propellant and thus reducing the formation of hot spots. Therefore, the addition of DP-2 to the propellant can significantly reduce mechanical sensitivity.

3.5. Rheological properties analysis

3.5.1. Capillary rheometer test

a. The effect of shear rate on apparent shear viscosity

In Fig. 13, the apparent shear viscosity (η) of blends was measured at 70 °C at different shear rates (γ). The viscosity of all samples decreases with increasing shear rate and all show pseudoplastic fluid characteristics. It could be ascribed to the enhanced shear effect when the shear rate increases, which destroyed the entanglement and physical cross-linked network structure between the nitrocellulose molecular chains. Additionally, the rate of this destruction is much greater than the rate of reconstruction, so the viscosity decreases. Moreover, it was evident that the viscosity of all samples exhibited an exponential relationship with shear rate (Wang et al., 2021), and the Ostwald de Wale power law model was adopted to describe the viscosity-shear rate relationship of the propellant (Ding et al., 2017; Zhang et al., 2022). The Ostwald de Wale power law model formula is as **Equation (2)**:

$$\eta = \frac{\tau}{\gamma} = K \times \gamma^{n-1} \tag{2}$$

Where η is apparent shear viscosity, Pa·s; K is the consistency factor; γ is the shear rate, s^{-1}; and n is the non-Newton index. The larger the

Table 2
The power-law model parameters of samples.

DP-2 content	$K \times 10^3$	$n-1$	n	R^2
0 wt%	13.27	−0.88	0.12	0.999
0.5 wt%	4.57	−0.70	0.30	0.998
1 wt%	4.38	−0.73	0.27	0.999
2 wt%	4.26	−0.74	0.26	0.999

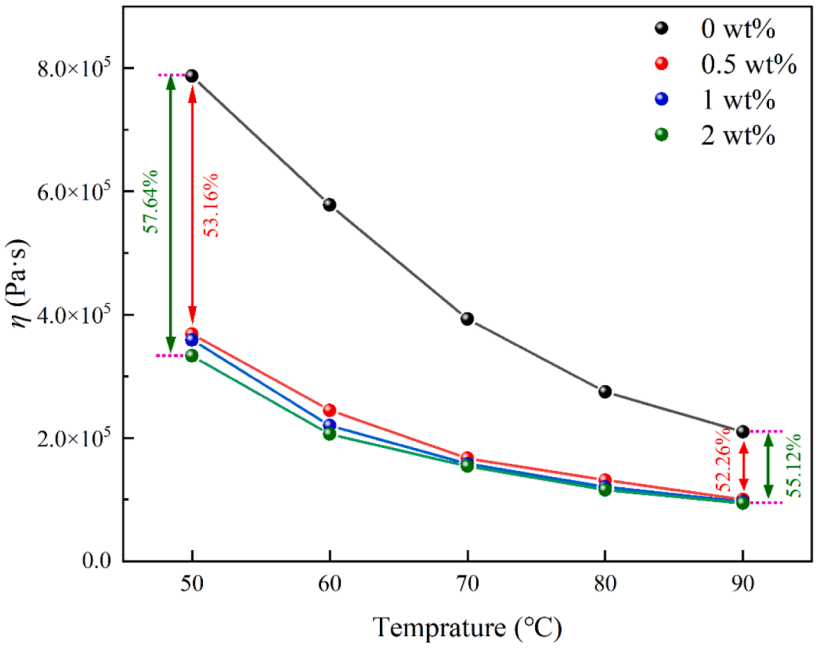

Fig. 14. The apparent shear viscosity of blends at different temperatures was tested at a shear rate ($\gamma = 4$).

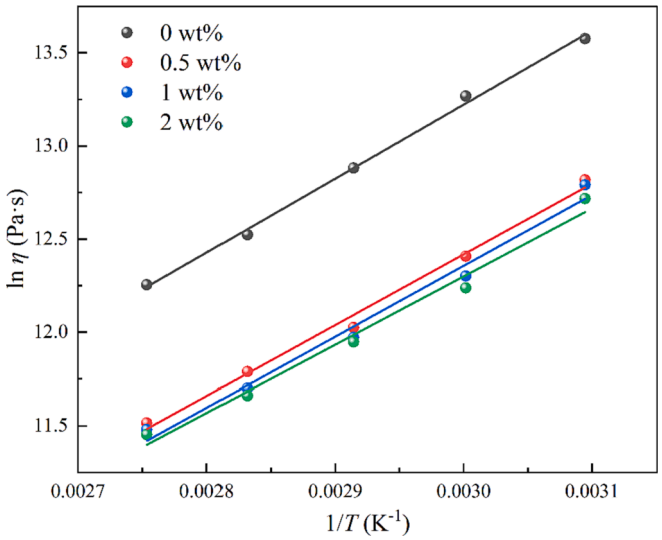

Fig. 15. The relationship between ln η and 1/T of blends.

Table 3
E_η of samples at a shear rate of 4.

DP-2 content	$E_\eta \times 10^5$	R^2
0 wt%	3.30	0.997
0.5 wt%	3.15	0.991
1 wt%	3.16	0.979
2 wt%	3.04	0.960

value of K, the greater the viscosity of the material, and the smaller the value of n, the greater the non-Newtonianity. $n < 1$, the material is pseudoplastic fluid, $n = 1$, Newton fluid, $n > 1$, swelling plastic fluid.

Apparently, the apparent shear viscosity of samples gradually decreased with the increase of DP-2 content. The power-law model parameters of samples were obtained by fitting the experimental data in Fig. 14 according to **Equation (2)**, and the results were shown in Table 2. As can be seen from Table 2, the K values of blends with different mass fractions of DP-2 decreased by 65.56 %, 66.99 %, and 67.90 %, respectively, compared with the blank sample.

b. The effect of temperature on apparent shear viscosity

In Fig. 14, the apparent shear viscosity of blends at different temperatures was tested at a shear rate ($\gamma = 4$). The apparent shear viscosity of blends gradually decreased with increasing temperature and exhibited a decrease in magnitude. This phenomenon could be attributed to the intensification of irregular thermal motion of molecules with rising temperature, resulting in increased molecular spacing and enhanced formation of free volume within the material. Consequently, chain segments experience greater ease in movement, leading to a decrease in intermolecular interactions and an increase in mobility.

Compared with blank sample, the apparent shear viscosity of blends with different mass fractions of DP-2 decreased by 53.16 %, 54.37 %, and 57.64 % at 50 °C; and decreased by 52.26 %, 53.93 %, and 55.12 % at 90 °C, respectively.

The relationship between the viscosity of the propellant and the temperature was in accordance with the Arrhenius equation (Zhang and Luo, 2021; Dinsdale and Quested, 2004), as in **Equation (3)**.

$$\eta = A\exp(E_\eta/RT) \tag{3}$$

Where T is temperature in K, Pa·s; A is the pre-exponential factor, R is the gas constant (8.314Jmol^{-1}K^{-1}) and E_η is the activation energy for viscous flow (J·mol^{-1}) and is used to characterize the dependence of viscosity on temperature.

Taking the natural logarithm of both sides of **Equation (3)** yields **Equation (4)**.

$$\ln\eta = \ln A + \frac{E_\eta}{R} \times \frac{1}{T} \tag{4}$$

The relationship curves between ln η and $1/T$ of blends were shown in Fig. 15, and the results were shown in Table 3.

Obviously, compared with blank sample, the activation energy for viscous flow of blends containing DP-2 was reduced. This indicates that the addition of DP-2 could reduce the temperature sensitivity of the propellant viscosity. The study on the activation energy for viscous flow of the propellant is of great significance to guide the production of the propellant.

3.5.2. *Torque rheometer test*

In Fig. 16, the screw torque and extrusion pressure were tested when the propellant blends were extruded at T_1 = 25 °C, T_2 = 45 °C, T_3 = 90 °C, 70 °C, and 50 °C respectively at a rotation speed of 3. The peak torque, peak extrusion pressure, balance torque and balance extrusion pressure data were summarized in Table 4. Among them, the data for blank sample was not collected due to excessive pressure in the screw at 50 °C and 70 °C, which caused the failure of the pneumatic pressure quick release clamp. As a result, propellant material leaked from the gap, leading to test failure.

According to previous studies, the balance torque of the screw can be used to characterize the viscosity (Belem and Ferraz, 2020; Freire et al., 2009; Hidalgo et al., 2012). It can be seen that the addition of DP-2 has greatly improved the flowability of the propellant. At 90 °C, the flow parameters of blends with DP-2 content of 0.5 wt%, 1 wt%, and 2 wt% were reduced by more than 50 % compared with blank sample. When the extrusion temperature was lowered to 70 °C, the flow parameters of blends with DP-2 content of 0.5 wt%, 1 wt%, and 2 wt% were still more than 40 % lower than those of blank sample at 90 °C. When the extrusion temperature was lowered to 50 °C, the flow parameters of blend with DP-2 content of 0.5 wt% were slightly higher than those of blank sample at 90 °C, but the flow parameters of blends with DP-2 content of 1 wt%, and 2 wt% were still lower than those of blank sample at 90 °C.

The test results from the capillary rheometer and torque rheometer indicated a remarkable decrease in both the apparent viscosity of the propellant and the torque of screw. It could be concluded that the flowability of the propellant was significantly enhanced by adding DP-2 to the propellant. This change in flowability suggested that DP-2, as a spherical compound with a multi-branched structure, could play a ball-like role in the propellant matrix, weaken the mutual entanglement between molecular chains of nitrocellulose. Moreover, this variation could also expand the free volume between molecular chains, and making it easier for molecular chain segments to slip. The mechanism of DP-2 improving fluidity could be briefly illustrated in Fig. 17.

3.6. *Mechanical property analysis*

The result of anti-impact strength test was shown in Fig. 18. When 0.5 wt% of DP-2 was added, the impact strength of the propellant was slightly improved, which may be due to the fact that DP-2 improved the flowability of the propellant, thus increasing the orientation of the molecular chain. Besides, it may be resulted from the formed hydrogen bonds were DP-2 molecules and nitrocellulose molecules, and DP-2 molecules formed a cross-linked structure with the propellant matrix through hydrogen bonds in the system. With the further increase of DP-2 content, a decreasing trend was observed, likely attributed to the absence of chain entanglement of dendrimer DP-2, resulting in reduced mechanical property when incorporated into the propellant.

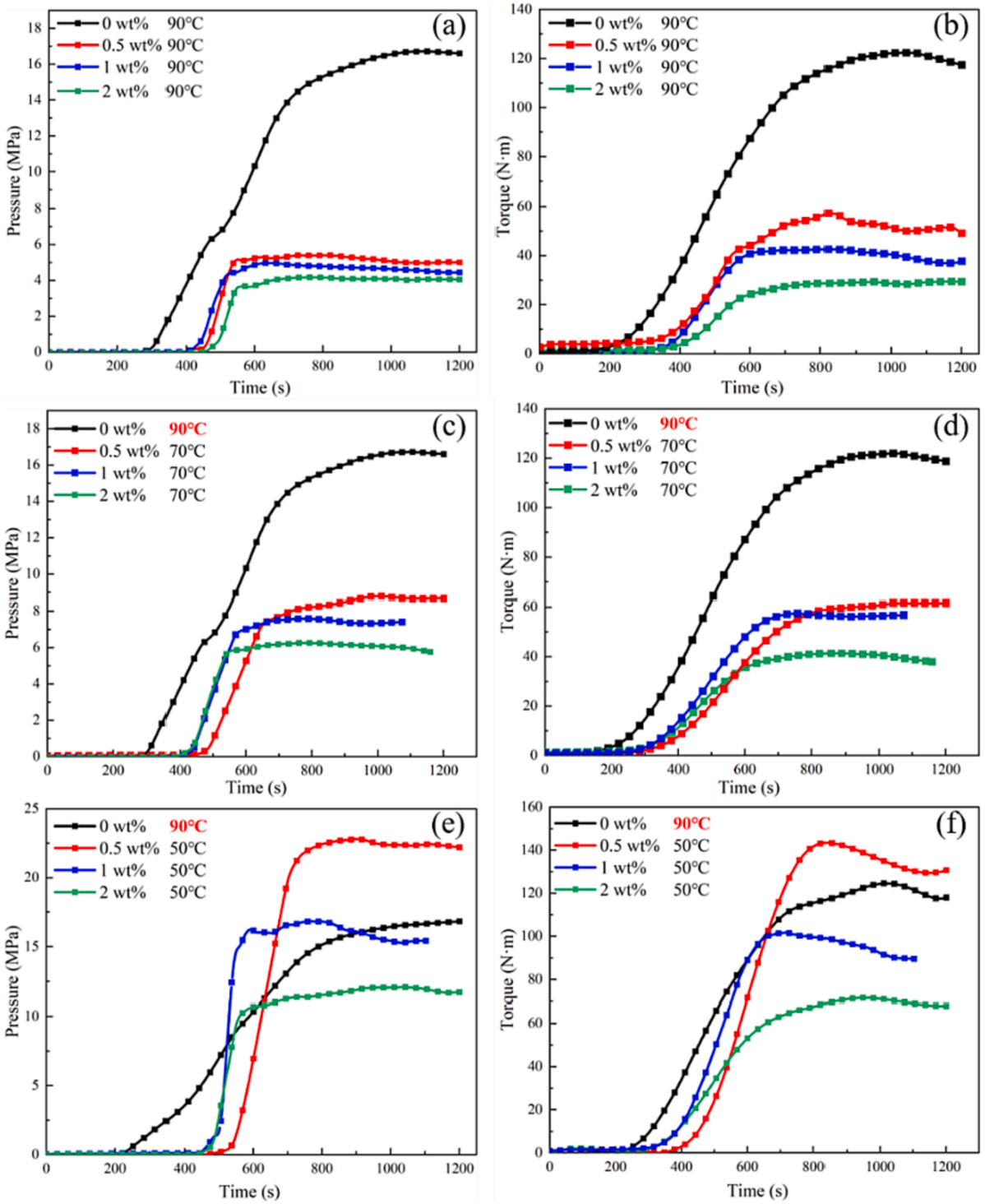

Fig. 16. The screw torque and extrusion pressure of the blends at 90 °C, 70 °C, and 50 °C at a rotation speed of 3.

3.7. Combustion characteristics

3.7.1. Combustion performance

The relationship between burning rate (u) and burning pressure (p) of the propellant was described by Vieille's rule (Trache et al., 2019), according to **Equation (5)**.

$$u = ap^n \tag{5}$$

Where a is the burning rate coefficient, a constant dependent on the chemical composition and the initial propellant temperature; n is the pressure exponent of the burning rate. To further study the burning behavior of the propellant, dynamic vivacity (L) and relative pressure (B) were calculated according to **Equation (6)** and **Equation (7)** (Xiao et al., 2016).

$$L = \frac{d_{p(t)}/dt}{p(t) * p_m} \tag{6}$$

$$B = \frac{p(t)}{p_m} \tag{7}$$

Table 4
Parameters of torque rheometer when the screw rotation speed was 3.

DP-2 content		0 wt%	0.5 wt%	1 wt%	2 wt%
P_1	90 °C	17.267	5.705	5.099	4.509
	70 °C	—	9.06	7.712	6.761
	50 °C	—	23.698	16.916	12.277
P_2	90 °C	16.573	5.023	4.567	4.003
	70 °C	—	8.625	7.405	6.077
	50 °C	—	22.474	15.831	11.842
M_1	90 °C	129.426	59.288	46.082	31.134
	70 °C	—	65.990	61.412	43.744
	50 °C	—	146.686	105.16	74.842
M_2	90 °C	121.707	50.557	39.943	28.174
	70 °C	—	60.852	56.112	40.471
	50 °C	—	134.248	94.521	69.975

In Fig. 19, from an overall perspective, according to the analysis of the smooth *L-B* curves in Fig. 19**d-f**, all samples burned stably without obvious abnormal combustion phenomena. The results indicated that the addition of DP-2 would not affect the combustion stability of the propellant. From Fig. 19**a-c**, and Fig. 19**g-i**, it was evident that an increase in DP-2 content leads to a gradual prolongation of the complete combustion time of the propellant and a decrease in burning rate. Conversely, elevating the initial temperature resulted in a reduction of burning time and an enhancement of the burning rate. These findings demonstrated that incorporating inert substances into the propellant retarded its combustion process, while raising the initial temperature enhanced its chemical activity.

As revealed by **Equation (5)**, there was a tight correlation and entanglement between the pressure exponent, combustion pressure, and combustion rate coefficient, and a tiny change in any of the experimentally measured variables could trigger considerable variations in the calculated combustion rate coefficient or pressure exponent. To further evaluated the influence of DP-2 on the combustion behavior of the propellant, the results of the maximum pressure, combustion rate coefficient, and pressure exponent during the combustion process of the propellant with different DP-2 content were presented in Fig. 20. From Fig. 20**a-b**, it could be observed that the maximum pressure and combustion rate coefficient gradually decrease with increasing DP-2 mass fraction. When lowering the temperature, the maximum pressure and burning rate also decrease. In Fig. 20**c**, the pressure exponent showed an overall increasing trend as the DP-2 mass fraction increased, but a slight decline was noticed in the propellant with 2 wt% of DP-2 at 20 °C and 50 °C. When the temperature was raised, the pressure index decreased.

3.7.2. *Energy performance*

The energy parameters of the propellant containing DP-2 were displayed in Table 5.

DP-2, an inert additive, caused a gradual decrease in the gunpowder impetus as the content increased. When the DP-2 content reached 2 wt %, its gunpowder impetus was 999.14 J/g, which was a 3.84 % decrease compared to blank sample.

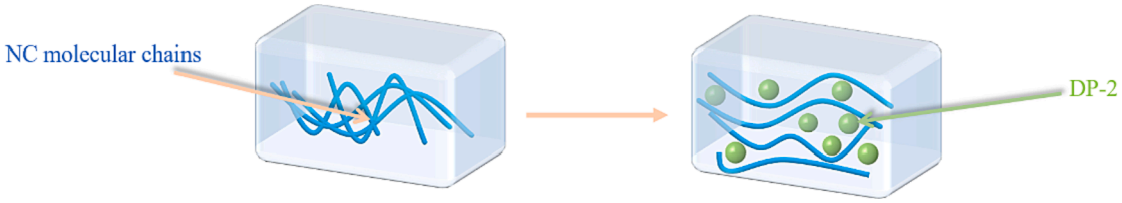

Fig. 17. The mechanism of DP-2 improving fluidity of the propellant.

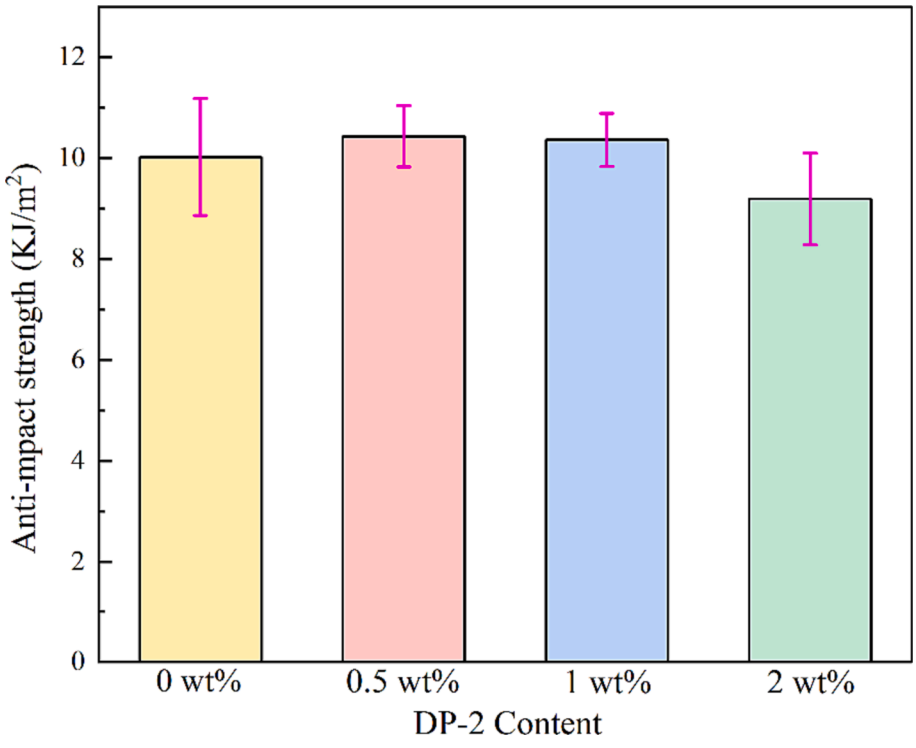

Fig. 18. The anti-impact strength of the propellant with different mass fraction of DP-2.

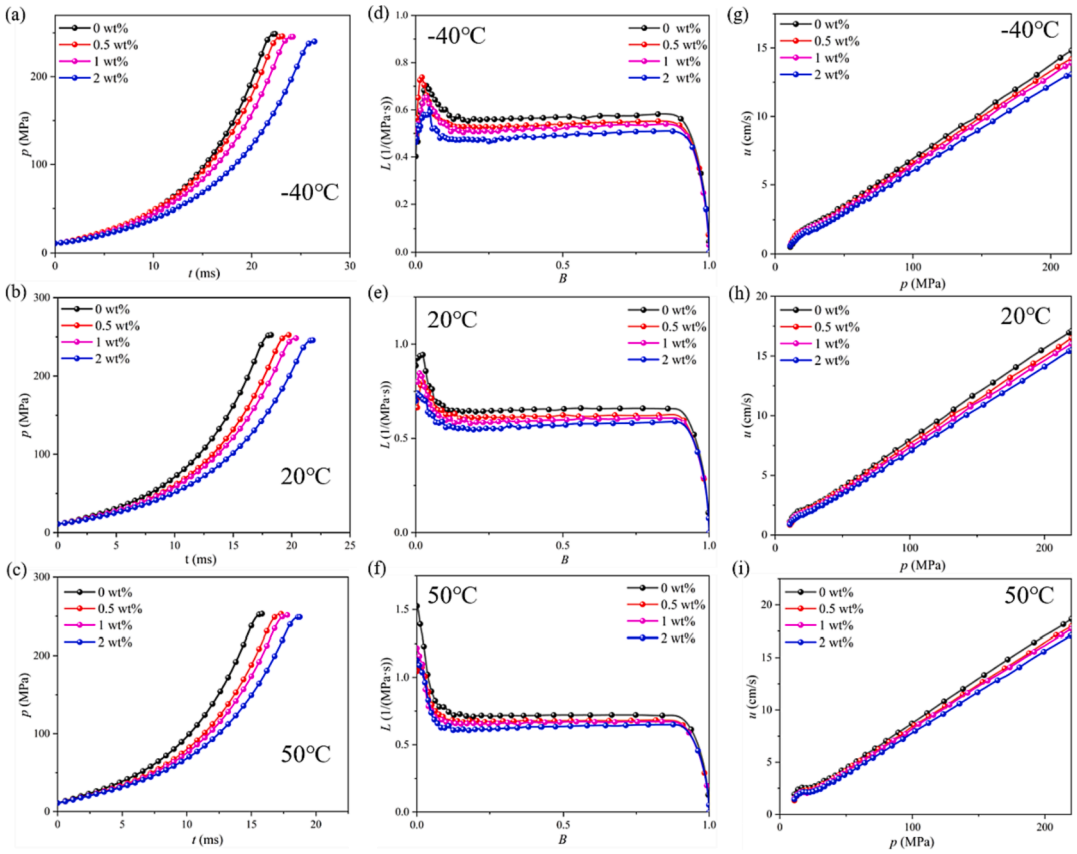

Fig. 19. The *p-t* (a-c), *L-B* (d-f) and *u-p* (g-i) curves at −40 °C, 20 °C and 50 °C of the propellant containing DP-2.

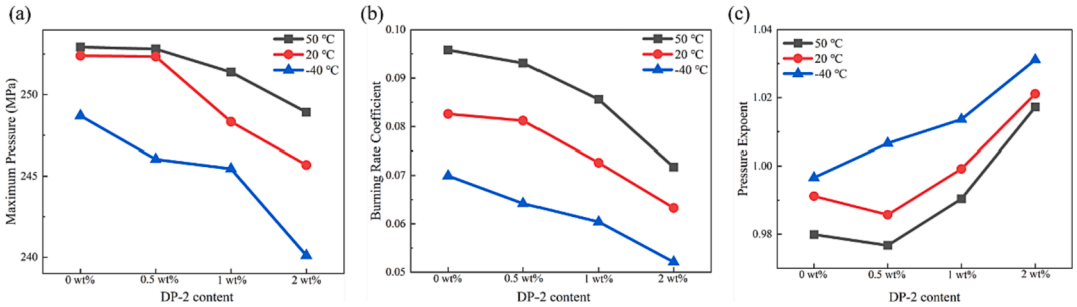

Fig. 20. The maximum pressure, burning rate coefficient, and pressure exponent of the propellant contaning DP-2 during the combustion process.

Table 5
The gunpowder impetus of the propellant containing DP-2.

DP-2 content (wt%)	The gunpowder impetus (J/g)	Percentage reduction (%)
0	1039.11	–
0.5	1019.82	1.86
1	1014.65	2.35
2	999.14	3.84

4 Conclusion

In summary, this study initially incorporated the dendrimer DP-2 into the propellant system, enabling investigation of its thermal decomposition, chemical stability, sensitivity, rheological properties, mechanical property, and combustion characteristics across varying concentrations. The result revealed that the flowability of the propellant was significantly improved with increasing DP-2 content. Therefore, a proper addition content of DP-2 can improve the thermal stability, chemical stability, sensibility, and mechanical properties of the propellant. Among them, there was a slight decrease in impact sensitivity when DP-2 was added at 2 wt%. Meanwhile, the addition of DP-2 would not influence the stable combustion behavior of the propellant, and the energy performance of the propellant containing DP-2 in terms of the gunpowder impetus would be somewhat diminished when compared to that of the blank sample. On the whole, the dendrimer DP-2 could serve as an effective processing aid to enhance the production safety of propellant during solventless extrusion processe, with a more suitable addition range of 0.5 wt%-1 wt%.

Declaration of competing interest

The authors declare that they have no known competing financial interests or personal relationships that could have appeared to influence the work reported in this paper.

Acknowledgments

This study thanks to Prof. Xiaoan Wei, Dr. Binbing Wang, Dr. Jinghao Liang, Engineer Yu Yannian, Engineer Yin Shenglai, and analysis and testing center of Nanjing University of Science and Technology for their experimental help and technical support. This research was supported by the Jiangsu Funding Program for Excellent Postdoctoral Talent (2023ZB472), and Project funded by China Postdoctoral Science Foundation (2023TQ0158).

References

Belem, B.R., Ferraz, H.G., 2020. Rheological profile in mixer torque rheometer of samples containing furazolidone and different binders. Chem. Eng. Res. Des. 160, 533–539.

Carter, R., 1988. A new purpose-built continuous processing facility for energetic materials. Propellants Explos. Pyrotech. 13 (3), 80–86.

Chen, L., Li, Q., Zhao, L., Nan, F., Liu, J., Wang, X., Chen, F., Shao, Z., He, W., 2022. Enhancement strategy of mechanical property by constructing of energetic RDX@CNFs composites in propellants, and investigation on its combustion and sensitivity behavior. Combust. Flame 244.

de Klerk, W.P.C., 2015. Assessment of stability of propellants and safe lifetimes. Propellants Explos. Pyrotech. 40 (3), 388–393.

Ding, Y., Wei, R., Ying, S., 2017. In-line rheological behaviors of gun propellant substitute assisted with supercritical CO2 in extrusion processing. Propellants Explos. Pyrotech. 42 (3), 247–252.

Dinsdale, A.T., Quested, P.N., 2004. The viscosity of aluminium and its alloys—A review of data and models. J. Mater. Sci. 39 (24), 7221–7228.

Dombe, G., Mehilal, D., Bhongale, C., Singh, P.P., Bhattacharya, B., 2015. Application of twin screw extrusion for continuous processing of energetic materials. Cent. Eur. J. Energ. Mater. 12 (3), 507–522.

Jim Fleming, Werner Rousseau, Martijn Zebregs, C.v. Driel, Solventless extrude double-base (EDB) propellant charges- a review of the properties, technology, and applications, International Journal of Energetic Materials and Chemical Propulsion 21(3) (2022) 13-46.

Freire, E., Bianchi, O., Monteiro, E.E.C., Reis Nunes, R.C., Forte, M.C., 2009. Processability of PVDF/PMMA blends studied by torque rheometry. Mater. Sci. Eng. C 29 (2), 657–661.

Fu, E.-F., Sun, N., Xiao, Z.-G., 2022. Effects of phase change material (PCM)-based nanocomposite additives on thermal decomposition and burning characteristic of high energy propellants containing RDX. Defence Technol. 18 (4), 557–566.

Hajizadeh, E., Todd, B.D., Daivis, P.J., 2014. Shear rheology and structural properties of chemically identical dendrimer-linear polymer blends through molecular dynamics simulations. J. Chem. Phys. 141 (19), 194905.

Hajizadeh, E., Todd, B.D., Daivis, P.J., 2015. A molecular dynamics investigation of the planar elongational rheology of chemically identical dendrimer-linear polymer blends. J. Chem. Phys. 142 (17), 174911.

Han, K., Zhang, X., Zhan, S., Yu, M., 2010. Simultaneously enhancing mechanical properties and melt flow ability of polyamide 6 by blending with a hyperbranched polymer. J. Macromol. Sci. Part B 50 (2), 225–235.

Hidalgo, J., Jiménez-Morales, A., Torralba, J.M., 2012. Torque rheology of zircon feedstocks for powder injection moulding. J. Eur. Ceram. Soc. 32 (16), 4063–4072.

Hong, Y., Cooper-White, J.J., Mackay, M.E., Hawker, C.J., Malmström, E., Rehnberg, N., 1999. A novel processing aid for polymer extrusion: Rheology and processing of polyethylene and hyperbranched polymer blends. J. Rheol. 43 (3), 781–793.

Kang, D., Kim, H.I., 2021. Improvement in nano-pattern replication of injection molding by polyamide/dendrimer blend. Polym. Eng. Sci. 61 (3), 822–829.

Kowalczyk, J.E., Malik, M., Kalyon, D.M., Gevgilili, H., Fair, D.F., Mezger, M., Fair, M., 2007. Safety in design and manufacturing of extruders used for the continuous processing of energetic formulations. J. Energ. Mater. 25 (4), 247–271.

Li, S.-Y., Li, Y., Ding, Y.-J., Liang, H., Xiao, Z.-L., 2023. One-step green method to prepare progressive burning gun propellant through gradient denitration strategy. Defence Technol. 22, 135–143.

Merino, S., Brauge, L., Caminade, A.-M., Majoral, J.-P., Taton, D., Gnanou, Y., 2001. Synthesis and characterization of linear, hyperbranched, and dendrimer-like polymers constituted of the same repeating unit. Chem. – Eur. J. 7 (14), 3095–3105.

Nunez, C.M., Chiou, B.-S., Andrady, A.L., Khan, S.A., 2000. Solution rheology of hyperbranched polyesters and their blends with linear polymers. Macromolecules 33 (5), 1720–1726.

Shen, J., Liu, Z., Xu, B., Liang, H., Zhu, Y., Liao, X., Wang, Z., 2019. Influence of carbon nanofibers on thermal and mechanical properties of NC-TEGDN-RDX triple-base gun propellants. Propellants Explos. Pyrotech. 44 (3), 355–361.

Trache, D., Maggi, F., Palmucci, I., DeLuca, L.T., Khimeche, K., Fassina, M., Dossi, S., Colombo, G., 2019. Effect of amide-based compounds on the combustion characteristics of composite solid rocket propellants. Arab. J. Chem. 12 (8), 3639–3651.

Wang, X., Liu, Z., Fu, Y., Zhu, Y., Chen, L., Yang, J., Chen, Q., Xu, B., Chen, F., Liao, X., 2021. Bio-inspired synthesis of RDX@polydopamine@TiO2 double layer core–shell energetic composites with reduced impact and electrostatic discharge sensitivities. Appl. Surf. Sci. 567.

Wang, S.-W., Song, X.-D., Wu, Z.-K., Xiao, L., Zhang, G.-P., Hu, Y.-B., Hao, G.-Z., Jiang, W., Zhao, F.-Q., 2021. Simulation of the plasticizing behavior of composite modified double-base (CMDB) propellant in grooved calendar based on adaptive grid technology. Defence Technol. 17 (6), 1954–1966.

Xiao, Z., Ying, S., Xu, F., 2016. Progressive burning performance of deterred oblate spherical powders with large web thickness. Propellants Explos. Pyrotech. 41 (1), 154–159.

Zhang, X., 1997. Double-base gunpowder. Beijing Institute of Technology Press, Beijing.

Zhang, J., Chen, L., Zhao, L., Jin, G., He, W., 2023. Experimental insight into interaction mechanism of 1H-tetrazole and nitrocellulose by kinetics methods and TG-DSC-FTIR analysis. J. Anal. Appl. Pyrol. 169.

Zhang, G., Luo, Y., 2021. Preparation, characterization and plasticizing GAP-ETPE propellants of azide hyperbranched copolymer. Chinese J. Energ. Mater. 29 (11), 1039–1048.

Zhang, W., Zhao, D., Dong, Z., Li, J., Zhang, B., Yu, W., 2022. The consistency factor and the viscosity exponent of soybean-protein-isolate/wheat-gluten/corn-starch blends by using a capillary rheometry. Molecules 27 (19).